Title: Glycolysis upregulation is neuroprotective as a compensatory mechanism in ALS

Authors:

Ernesto Manzo[1], Ileana Lorenzini[4], Dianne Barrameda[1], Abigail G. O'Conner[1], Jordan M. Barrows[1], Alexander Starr[4], Tina Kovalik[4], Dakotah D. Shreiner[1], Archi Joardar[1], Jean-Charles Liévens[5], Robert Bowser[4], Rita Sattler[4], Daniela C. Zarnescu[1,2,3,*]

Affiliations:

1 Department of Molecular and Cellular Biology,

2 Department of Neuroscience

3 Department of Neurology, University of Arizona, Tucson, AZ 85721, USA

4 Neurology, Barrow Neurological Institute, Phoenix, AZ

5 Université de Montpellier, MMDN U1198, CC105, Place Eugène Bataillon, 34095 Montpellier Cedex 5, France.

* corresponding author

Abstract:

Amyotrophic Lateral Sclerosis (ALS), is a fatal neurodegenerative disorder, with TDP-43 inclusions as a major pathological hallmark. Using a *Drosophila* model of TDP-43 proteinopathy we found significant alterations in glucose metabolism including increased pyruvate, suggesting that modulating glycolysis may be neuroprotective. Indeed, a high sugar diet improves locomotor and lifespan defects caused by TDP-43 proteinopathy in motor neurons or glia, but not muscle, suggesting that metabolic dysregulation occurs in the nervous system. Overexpressing human glucose transporter GLUT-3 in motor neurons mitigates TDP-43 dependent defects in synaptic vesicle recycling and improves locomotion. Furthermore, *PFK* mRNA, a key indicator of glycolysis to be upregulated in flies and patient derived iPSC motor neurons with TDP-43 pathology. Surprisingly, *PFK* overexpression rescues TDP-43 induced locomotor deficits. These findings from multiple ALS models show that mechanistically, glycolysis is upregulated in degenerating motor neurons as a compensatory mechanism and suggest that increased glucose availability is protective.

Introduction

Amyotrophic lateral sclerosis (ALS) is a neurodegenerative disease affecting upper and lower motor neurons resulting in progressive muscle weakness and eventual death (Hardiman et al. 2017). Cellular metabolic defects arise early, and contribute to the clinical manifestation of systemic defects that include weight loss, dyslipidemia, and hypermetabolism (reviewed in (Dupuis et al. 2011; Joardar, Manzo, and Zarnescu 2017). However, it is unclear how metabolic defects relate, or may contribute to motor neuron degeneration.

Observations from both patients and animal models have begun to elucidate the mechanisms that contribute to metabolic defects in ALS. Interestingly, the human brain relies on glucose as its major energy source, and consumes ~20% of the body's glucose derived energy (Mergenthaler et al. 2013). Glucose defects have been previously reported in the frontal lobe and the cortex in ALS patients (Ludolph et al. 1992), and in mutant SOD1 mouse models of ALS (Browne et al. 2006; Miyazaki et al. 2012). Increased glucose availability has also been shown to reduce protein misfolding and delay neuronal degeneration in C. elegans models of neurodegeneration (Tauffenberger et al. 2012). In a recent pilot study, a high caloric diet based on high carbohydrate content has been shown to be well tolerated by patients, and reduce serious adverse events in ALS patients (Wills et al. 2014a). Taken together, these findings suggest that although defective glucose metabolism is still poorly understood in ALS, there lies a great opportunity to better understand its relationship to disease and explore its potential as a therapeutic avenue.

Our lab has developed a *Drosophila* model of ALS based on overexpression of human TDP-43 that recapitulates multiple disease aspects including cytoplasmic aggregates, neuromuscular junction (NMJ) abnormalities, lifespan, and locomotor defects (Estes et al., 2011, 2013). Importantly, the large majority of ALS patients (>97%) harbor TDP-43 cytoplasmic aggregates regardless of etiology, highlighting the importance of understanding TDP-43 toxicity mechanisms (Ling, Polymenidou, and Cleveland 2013; Neumann et al. 2006). Here, we report that in a *Drosophila* model of TDP-43 proteinopathy, glycolytic metabolites and genes are altered, and are consistent with increased glucose consumption. Moreover, key genes

responsible for driving glucose metabolism are upregulated in both patient derived induced pluripotent stem cell (iPSC) motor neurons and postmortem patient spinal cord tissue. In a fly model of TDP-43 proteinopathy, increased dietary glucose improves locomotor function and increases lifespan when TDP-43 is expressed in the central nervous system but not muscles. Additionally, genetic over-expression of human glucose transporters improves locomotor function, mitigates neuromuscular junction defects, and improves lifespan in a variant dependent manner. Finally, motor neuron overexpression of PFK, the rate limiting enzyme in glycolysis, improves locomotor function, suggesting that upregulation of glycolysis is neuroprotective through a compensatory mechanism in ALS. Together, our results show that increased glucose availability protects motor neurons and improves overall outcome in models of TDP-43 proteinopathy.

Results

Glycolysis and pentose phosphate pathways are altered by TDP-43 expression in motor neurons

To decipher metabolic alterations in ALS, we employed a *Drosophila* model of TDP-43 proteinopathy that recapitulates key features of the human disease including locomotor dysfunction and reduced survival (Estes et al. 2011; Estes et al. 2013). We conducted metabolomic profiling in whole third instar larvae expressing TDP-43 in motor neurons (D42>TDP-43^{WT} or D42>TDP-43^{G298S}) and controls (D42>w^{1118}). These experiments showed significantly increased phosphoenolpyruvate (PEP) and pyruvate in both TDP-43^{WT} and TDP-43^{G298S} suggesting an increase in glucose metabolism (PEP, P_{value} = 0.034 and pyruvate, P_{value} = 0.007 for TDP-43^{WT}; PEP, P_{value} =0.002 and pyruvate, P_{value} = 0.009 for TDP-43^{G298S}; see Fig.1 and Table 1). In larvae expressing TDP-43^{G298S}, we also found a decrease in ribulose/xylulose 5-phosphate (P_{value} = 0.011) in conjunction with increased sedoheptulose 7-phosphate (P_{value} = 0.008) suggesting that increased glycolytic input into the Pentose Phosphate Pathway occurs in a variant dependent manner (see Fig. 1, Table 1). Taken together these findings suggest that

glucose metabolism is altered in the context of TDP-43 proteinopathy, consistent with previous reports of metabolite alterations in plasma isolated from ALS patients (Lawton et al. 2012).

Key glycolysis and pentose phosphate pathway enzymes are upregulated by TDP-43 expression in motor neurons

An increase in glycolytic metabolites suggests a possible increase in glycolysis. To test this hypothesis, we profiled the expression of multiple enzymes known to regulate flux through glycolysis and the Pentose Phosphate Pathway. Phosphofructokinase-1 (PFK1; PFK in *Drosophila*) levels are considered to be rate-limiting for glycolysis, thus PFK expression provides a reliable determinant of flux for glucose breakdown (Tanner et al. 2018).

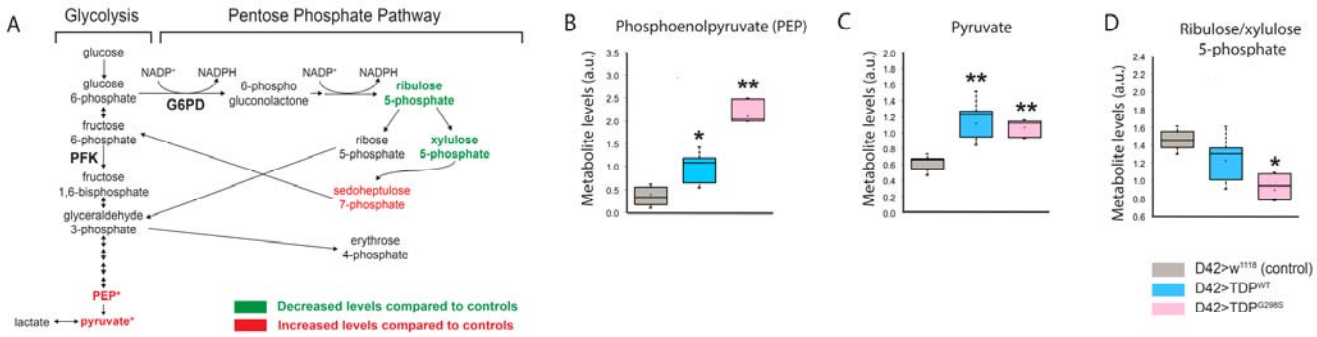

Figure 1. **Glycolysis and pentose phosphate pathways are altered by TDP-43 expression in motor neurons. (A)** Metabolite changes in glycolysis for whole larvae expressing TDP-43^{WT} or TDP-43^{G298S} were analyzed using mass spectrometry (see Materials and Methods). Green and red font represent metabolites that are significantly changed compared to controls (w^{1118}), as indicated. PEP and pyruvate were upregulated in both TDP-43^{WT} and TDP-43^{G298S} expressing flies (**B, C)**. One-way ANOVA was used to identify metabolites that differed significantly between experimental groups (N=5).

Altered metabolites in third instar larvae crossed with the motor neuron driver D42 GAL4 were measured using gas or liquid chromatography followed by mass spectrometry. Red and green colored cells indicate statistically significant changes (P_{value}<0.05) that are increased and decreased, respectively. Light red and light green colored cells indicate upward or downward trends, respectively (P_{value} <0.1).

To measure the levels of PFK in the context of TDP-43 proteinopathy we performed qPCR in ventral nerve chords dissected from third instar larvae expressing TDP-43^{WT} or TDP-43^{G298S} in motor neurons (D42>TDP-43) and w^{1118} controls. These experiments showed that PFK transcript levels are increased in the context of TDP-43^{WT} or TDP-43^{G298S}, albeit statistical significance was only achieved in the mutant TDP-43 (37% increase, P_{value} = 0. 06 for TDP-43^{WT} and 59% increase, P_{value} = 0. 0.014 for TDP-43^{G298S}; see Fig. 2A). These results suggest that flux through glycolysis is significantly increased in motor neurons in the context of TDP-43^{G298S}.

Finally, glucose-6-phosphate dehydrogenase (G6PD; Zw in *Drosophila*) was selected due to its role as the commitment step for the pentose phosphate pathway (PPP). Zw transcript levels are increased in TDP-43^{G298S} conditions (37% increase, P_{value} = 0.012, see Fig. 2B) consistent with increased glycolytic influx through the PPP in the context of mutant TDP-43.

PFK transcript is upregulated in human tissue

To confirm that the changes in our *Drosophila* model of ALS have clinical relevance, we assayed the transcript levels of PFK in human tissues and patient derived iPSC motor neurons. Humans have three isoforms of PFK, namely PFKM, PFKL, and PFKP. Although all are present in the brain, PFKL is expressed at low levels (Human Brain Transcriptome: http://hbatlas.org/) thus we focused on PFKP and PFKM. For human tissues we used spinal cords isolated from ALS patients with TDP-43 proteinopathy and controls lacking neurological defects (see Supplemental Table 2 for demographic information). qPCR experiments show that both PFKP and PFKM levels are significantly increased in human spinal cords (PFKP: 89% increase, P_{value} <0.001; PFKM: 55% increase, P_{value}=0.046, Fig. 2B). iPSC motor neurons were derived from a patient harboring the TDP-43 G298S mutation and differentiated as previously described (Coyne et al. 2017). qPCR profiling from iPSC derived motor neurons differentiated for 69 days showed a 91% increase in PFKP (P_{value}=0.018; see Fig. 2D) while no change was detected in PFKM. These experiments show that glycolysis is also upregulated in patient spinal cords and motor neurons consistent with our findings in the fly model. Similarly, G6PD transcript levels are increased by 49% in spinal cords of ALS patients (P_{value}=0.037; see Fig. 2C).

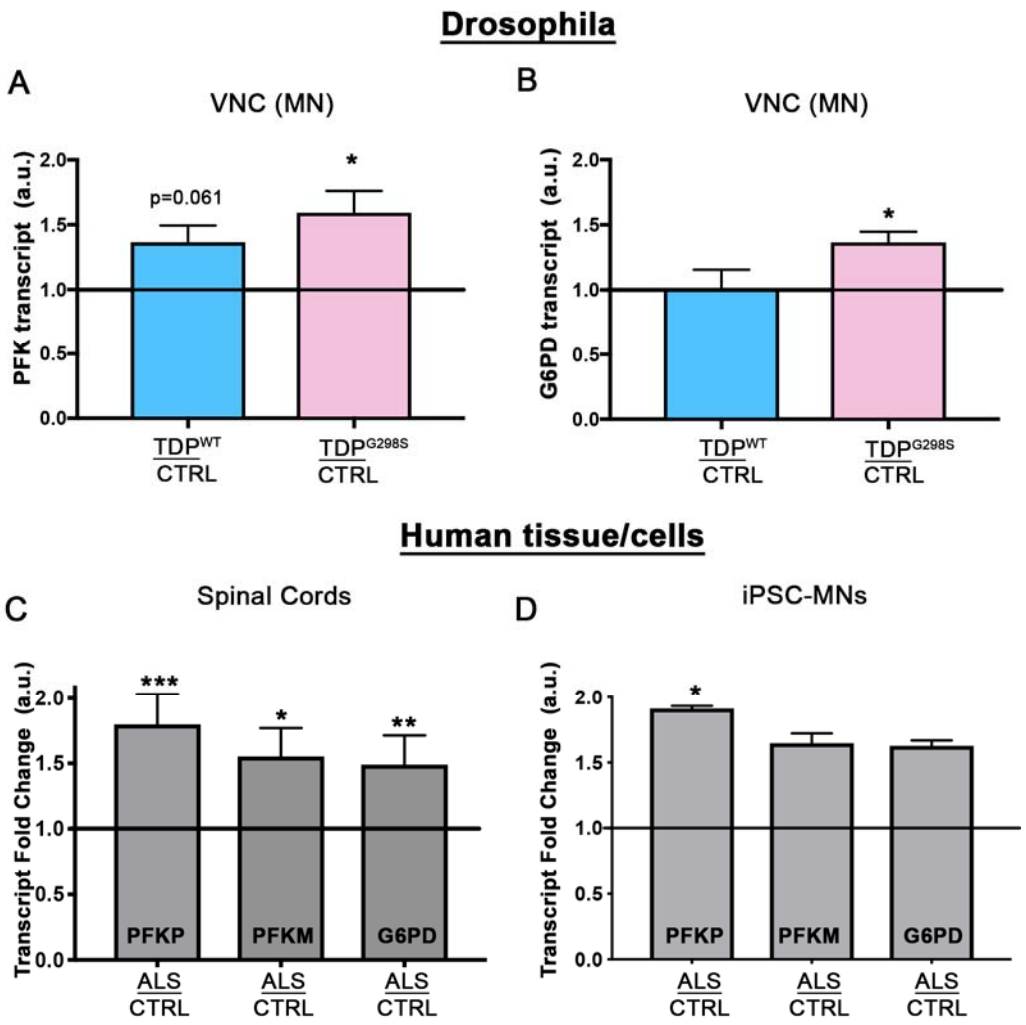

Figure 2. Glycolytic enzymes are transcriptionally upregulated. qPCR profiling of PFK (**A**; N=5) and G6PD (**B**; N=5) from ventral nerve cords of *Drosophila*. Human PFKP, PFKM, or G6PD mRNA levels were profiled in either spinal cords (**C**; N=8 control and 9 ALS cases) or human iPSCs (**D**; N=2). Kruskal-Wallis test was used to identify significance.

TDP-43 proteinopathy alters the capacity of motor neurons to import glucose

Our findings that TDP-43 expression in motor neurons alters glycolysis could be explained by and effect on glucose flux. To evaluate the levels of glucose in motor neurons, in the context of TDP-43 proteinopathy, we used a genetically encoded, FRET based, glucose sensor, FLII12Pglu-700μδ6 (Takanaga, Chaudhuri, and Frommer 2008; Fehr et al. 2003). The sensor comprises a bacterial glucose-sensing domain and a pair of cyan and yellow fluorescent

proteins that upon glucose binding, undergoes a conformational change and allows FRET to occur (Fig. 3A). This genetically encoded sensor has been previously used in conjunction with the GAL-UAS system in *Drosophila* to detect glucose flux and distribution in various cell types within the fly ventral nerve cord (Volkenhoff et al. 2018).

Upon stimulation with glucose, neurons expressing the glucose sensor alone or together with TDP-43 showed a small but significant increase in the FRET/CFP ratio (Figs. 3B, C). TDP-43^{WT} expressing neurons showed no significant difference in the FRET/CFP signal compared to controls (Figs. 3B, C, P_{value} <0.99). In contrast, TDP-43^{G298S} expressing neurons showed a significant increase in the FRET/CFP signal compared to controls (Figs. 3B, C, P_{value} <0.001). These results suggest that glucose flux is enhanced in TDP-43^{G298S} expressing neurons, and further substantiate our findings that glycolysis and the pentose phosphate pathway are significantly increased in the context of TDP-43 proteinopathy.

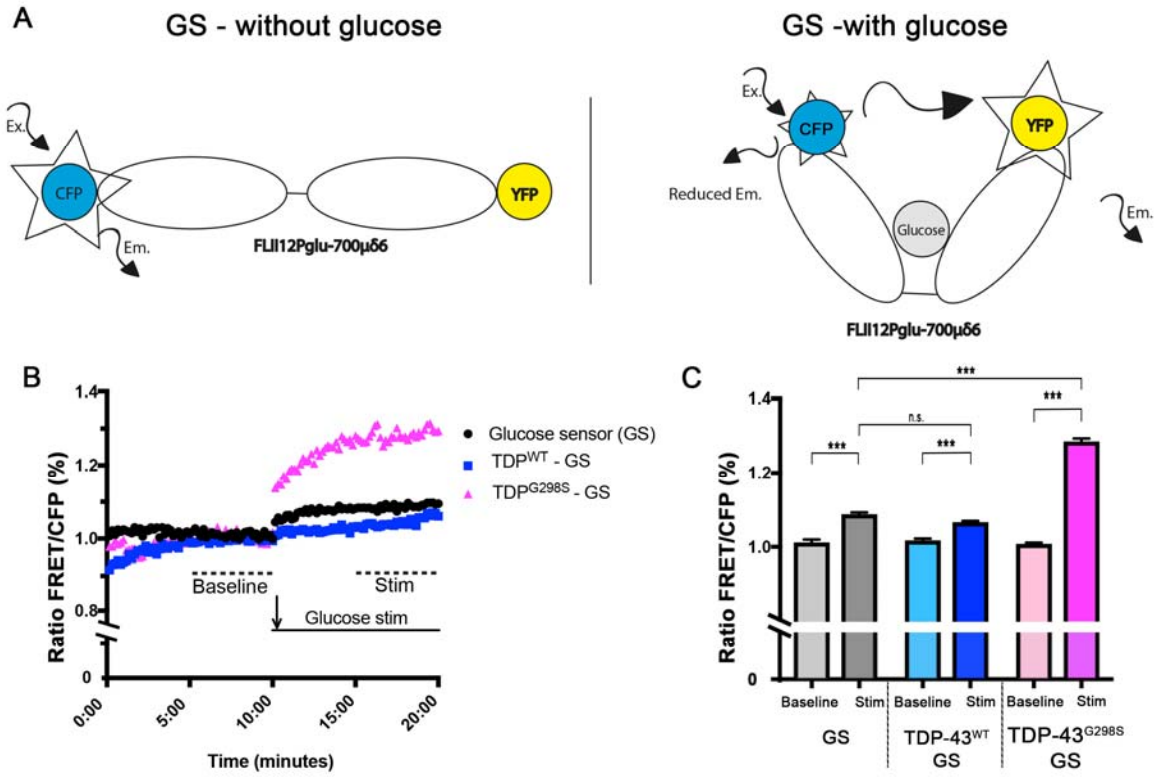

Figure 3. TDP expressing neurons have altered capacity to import glucose. FRET based glucose sensor described in (Volkenhoff et al. 2018) was used to measure the glucose import capacity. Glucose sensor schematic described in **(A)**. Ex – Excitation; Em – Emission.

Figure 3 (cont.) (B, C) TDP-43 expressing neurons and controls were imaged to detect CFP and FRET signal. 12-14 neurons were imaged every 10 seconds for 20 minutes. Values shown are the mean of 12-14 individual cells (ROI) from two ventral nerve cords. Kruskal-Wallis test was used to calculate significance.

A high glucose diet mitigates neuronal and glial induced TDP-43 toxicity

The alterations in glucose metabolism we have uncovered here could be a direct consequence of TDP-43 proteinopathy or alternatively, could reflect a coping mechanism. To distinguish between these two scenarios, we fed TDP-43 expressing flies a high glucose diet. As we have previously shown, the neuronal or glial expression of TDP-43^{WT} or TDP-43^{G298S} caused locomotor defects as indicated by increased larval turning time compared to controls (Estes et al. 2011; Estes et al. 2013). Of note, a high glucose diet increased the larval turning time of control larvae, consistent with previous reports that high sugar intake induces insulin resistance and obesity in flies (Musselman et al. 2011; Na et al. 2013). In contrast, a high glucose diet improved the larval locomotor defect caused by either neuronal, or glial expression of TDP-43 (Fig. 4A and Supplemental Fig. 4A). Interestingly, we found that increasing the concentration of glucose five-fold or higher rescued locomotor phenotypes caused by TDP-43 while no improvement was observed when glucose is only increased by two-fold (Supplemental Fig. 4A). Next, we examined the effect of glucose on lifespan and found that the reduced survival caused by neuronal or glial expression of TDP-43^{WT} or TDP-43^{G298S} was also significantly improved by feeding *Drosophila* a high sugar (HS) versus a regular sugar (RS) diet (23.5 days for TDP-43^{WT} on RF and 53 days for TDP-43^{WT} on HS, P_{value} = <0.0001; 14.5 days for TDP-43^{G298S} on RS and 41 days for TDP-43^{G298S} HS, P_{value} = <0.0001 ; Fig. 4B, Supplemental Fig. 4B). Together, these results suggest that while a high sugar diet is detrimental to control flies, it improves key hallmarks of motor neuron disease including locomotor dysfunction and reduced survival in a dose dependent manner.

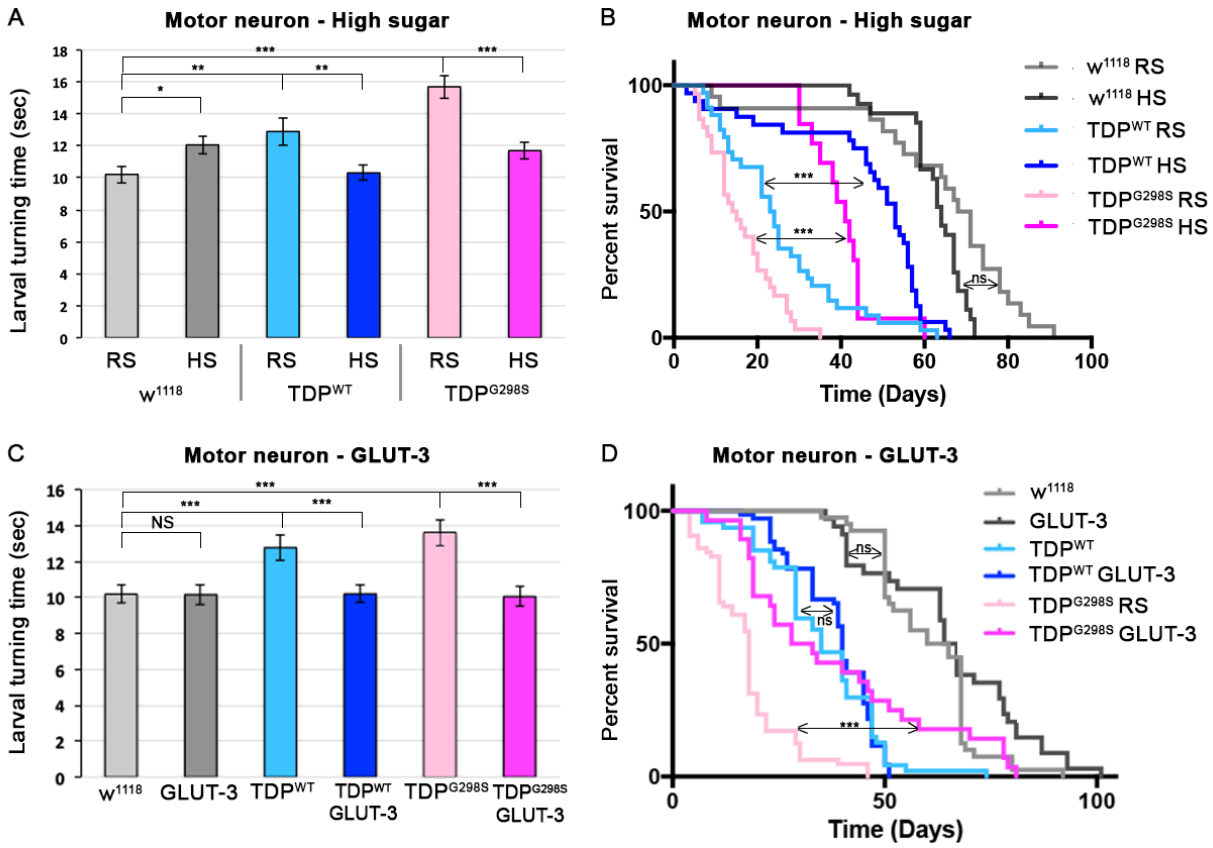

Figure 4. A high glucose diet rescues neuronal TDP-43 toxicity in flies. TDP-43^{WT} or ALS associated TDP-43^{G298S} were expressed in MNs (using GAL4-UAS). **(A, B)** Larval turning and lifespan assays for *Drosophila* fed a corn meal based food containing either regular concentration of sugar (RS) or a high sugar diet (HS:10x the standard amount of sugar). **(C, D)** Larval turning and lifespan assays for *Drosophila* expressing GLUT-3 on its own or with TDP-43, as indicated. At least 30 larvae were tested in larval turning assays and on average 20 adults were assayed for survival. Kruskal-Wallis test and Log-rank (Mantel-Cox) test was used to determine statistical significance for larval turning and survival curve respectively. * - $p < .05$, ** - $p<0.01$, *** - $p<0.001$.

Overexpression of human glucose transporters mitigate TDP-43 dependent phenotypes in neurons or glia

Our results on a high sugar diet suggest that increased glucose availability is protective in our fly model of ALS. However, because feeding can cause systemic effects and to further probe the role of glucose in our *Drosophila* model of ALS, we co-expressed TDP-43 and the human

glucose transporter GLUT-3 in motor neurons or glia. GLUT-3 is the primary glucose transporter of mammalian neurons, and has a high capacity for glucose (Ferreira, Burnett, and Rameau 2011). Co-expression of GLUT-3 and TDP-43^{WT} or TDP-43^{G298S}, in either motor neurons or glia cells, improved the locomotor deficits caused by TDP-43 expression alone (Fig. 4C). Moreover, GLUT-3 expression in neurons improved the locomotor ability of adult flies expressing TDP-43^{WT} or TDP-43^{G298S} (as measured by negative geotaxis assays, Supplemental Figure 4D). When using the standard log-rank test for analyzing the survival data, lifespan was significantly increased when GLUT-3 was co-expressed with TDP-43^{G298S} in motor neurons, but not glial cells (18 days for TDP-43^{G298S} and 30 days for TDP-43^{G298S}, P_{value} = <0.0001). However, when using the Mantel-Cox test, which weighs earlier deaths more significantly, we found that GLUT-3 overexpression increases lifespan when TDP-43^{G298S} is expressed in glial cells (43.5 days vs 51.5 days, P_{value} = 0.015**). GLUT-3 had no effect on lifespan when TDP-43^{WT} was expressed in either motor neurons or glia. These findings suggest that increased glucose availability is protective in both motor neurons and glia but to a different extent that likely reflects different metabolic capabilities of the two cell types.

Although GLUT-3 is the predominant glucose transporter in the brain, recently, the human glucose transporter GLUT-4, an insulin dependent glucose transporter expressed primarily in muscle has been shown to localize to the plasma membrane to support synaptic activity (Ashrafi et al. 2017). To test whether GLUT-4 also modulates TDP-43 proteinopathy, we co-expressed GLUT-4 and TDP-43 in either motor neurons or glia. Similar to GLUT-3, co-overexpression of GLUT-4 and TDP-43^{WT} or TDP-43^{G298S}, in either motor neurons or glial cells, improved the locomotor deficits caused by TDP-43 expression alone (Supplemental Figure 4C). Interestingly, lifespan was not significantly increased for either glial or motor neuron expression, suggesting that constitutive increase in glucose availability mediated by GLUT3 is more potent in suppressing TDP-43 proteinopathy in flies (Supplemental Figure 4C). Notably, while TDP-43 overexpression in muscle causes larval turning phenotypes, co-overexpression of either GLUT-3 or GLUT-4 in muscle does not mitigate TDP-43 dependent locomotor deficits, suggesting that the primary metabolic defect lies in the nervous system (Supplemental Figure 4C).

TDP-43 dependent defects at the neuromuscular junction are rescued by GLUT-3

We previously described defects at the *Drosophila* neuromuscular junction (NMJ) caused by neuronal expression of TDP-43. These defects include a reduction in synaptic bouton number (Coyne et al. 2014; Estes et al. 2013) and a reduction in synaptic vesicle endocytosis as indicated by FM1-43 dye uptake experiments (Coyne et al. 2017). To test whether increased GLUT-3 could also rescue morphological and functional defects at the larval NMJ, we co-expressed GLUT-3 and TDP-43 in motor neurons. Co-expression of GLUT-3 rescued NMJ size as indicated by the total number of synaptic boutons in both TDP-43^{WT} (P_{value} = 0.004) and TDP-43^{G298S} (P_{value} = 0.023) expressing larvae (Figs. 5A and 5C). Moreover, GLUT-3 overexpression partially restores synaptic vesicle endocytosis deficits caused by TDP-43 (Figs. 5B and 5D, P_{value} <0.001 for both TDP-43^{WT} and TDP-43^{G298S}). Taken together, these results show that GLUT-3 expression in motor neurons mitigates morphological and functional defects caused by TDP-43 at the NMJ and suggest that increased glucose availability in motor neurons is neuroprotective in ALS.

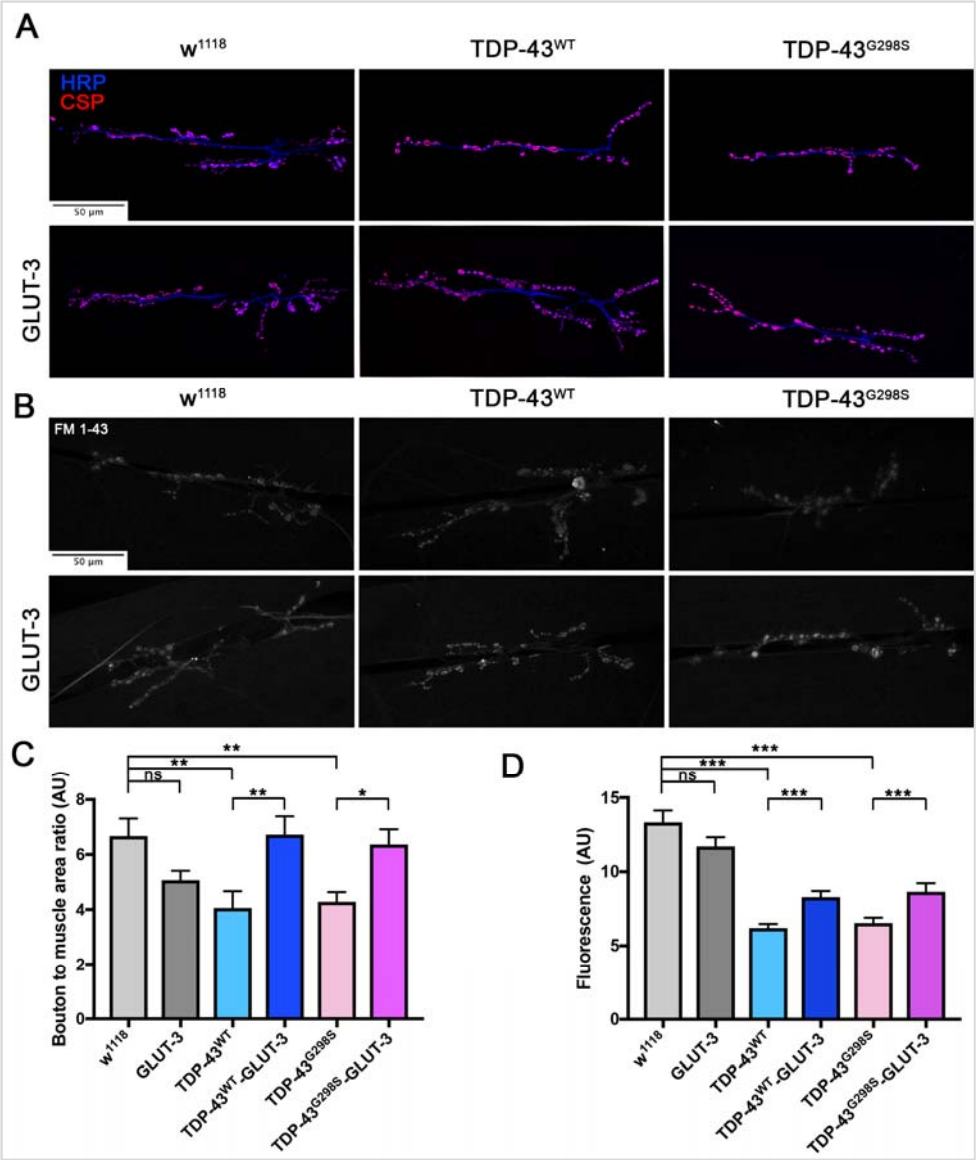

Figure 5. TDP-43 dependent defects at the NMJ are rescued by GLUT-3. Third instar larvae NMJ from segment A3, muscle 6/7 were immunostained for CSP and HRP **(A)** or analyzed for their ability to endocytose FM1-43 dye upon stimulation with 90 mM KCl.

Figure 5 (cont.) (A, C) Neuronal TDP-43 expression in *Drosophila* neurons reduces the number of boutons (labeled with CSP and HRP **A, C**) and reduces FM1-43 dye uptake **(B, D)**. These morphological **(A, C)** and functional **(B, D)** deficits are rescued by co-expression of GLUT-3. N = 7-10 larvae. Kruskal-Wallis test was used to identify significance.

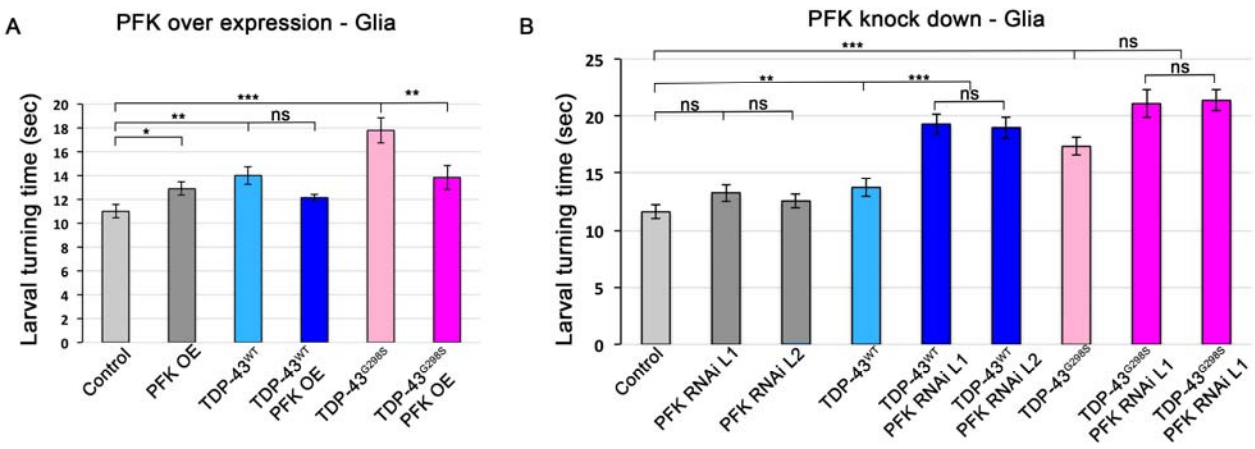

Figure 6. Co-overexpression of PFK rescues TDP-43 induced locomotor defects. TDP-43^{WT} or ALS associated TDP-43^{G298S} were expressed in MNs (using the Gal4-UAS system together with *Drosophila* UAS-PFK). N = 30 larvae. Kruskal-Wallis was used to determine statistical significance. * - $P_{value} < .05$, ** - $P_{value} < 0.01$, *** - $P_{value} < 0.001$.

Neuronal co-expression of PFK rescues TDP-43 induced toxicity

Increased PFK levels in conjunction with our findings that increased glucose availability is protective suggest that increased glycolysis may be compensatory. To test this hypothesis we directly manipulated glycolysis genetically, either via PFK overexpression or RNAi knock-down, in the context of TDP-43 proteinopathy. Over expression of PFK alone in motor neurons negatively altered locomotor activity suggesting that in normal neurons high glycolytic activity may be toxic (Fig. 6A). However, the co-expression of PFK with TDP-43^{WT} or TDP-43^{G298S} rescued locomotor defects to control levels ($P_{value} = 0.003$ for TDP-43^{WT} and $P_{value} <0.001$ for TDP-43^{G298S}, Fig. 6A). In contrast, PFK RNAi knock-down had no significant effect on larval turning when expressed in motor neurons alone (53% knock-down, $P_{value}= 0.04$, see Materials and Methods). However, when PFK was knocked down by RNAi in the context of TDP-43 proteinopathy we found that it significantly increased larval turning times for TDP-43^{WT} albeit it had no effect on TDP-43^{G298S} ($P_{value} < 0.001$ for TDP-43^{WT} and $P_{value} = 0.767$ for TDP-43^{G298S}, Fig. 6B). One possible interpretation for this variant dependent effect is that the metabolic deficit of TDP-43^{G298S} is so severe that it may be difficult to exacerbate by further altering energy

metabolism. Of note, a second PFK RNAi line (y(1) sc[*] v(1); P{y[+t7.7] v[+t1.8]=TRiP.HMS01324}attP2) was tested, but was lethal when expressed in motor neurons.

Similar to the experiments with motor neurons, the over-expression of PFK in glial cells causes a locomotor defect, while the expression of two independent PFK RNAi lines has no effect on locomotor activity as determined by larval turning assays (Supplemental Fig. 6). When PFK is co-expressed in glial cells with TDP-43^{WT} there is a slight but not statistically significant reduction in larval turning ($P_{value} > 0.302$) while it significantly mitigates TDP-43^{G298S} ($P_{value} = 0.001$, Supplemental Fig. 6). Moreover, the knockdown of PFK in conjunction with TDP-43^{WT} significantly impaired locomotor function when compared to TDP-43^{WT} expression alone ($P_{value} < 0.001$, Supplemental Fig. 6). PFK knock down did not affect TDP-43^{G298S} expressing flies $P_{value} > 0.057$, Supplemental Fig. 6). These results indicate that an increase in glycolysis, in either motor neurons or glial cells, can ameliorate TDP-43 toxicity.

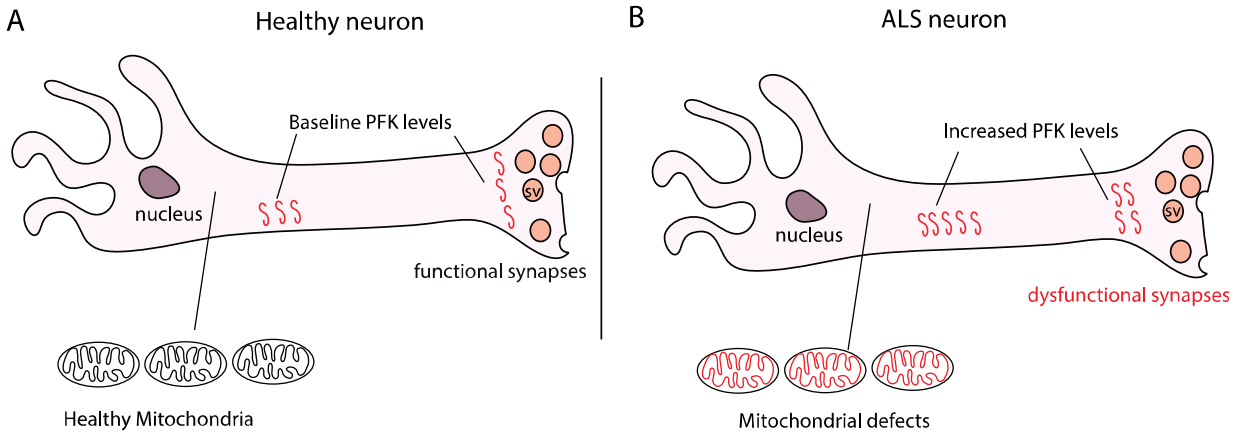

Figure 7. Proposed model showing PFK transcript levels increase in response to TDP-43 proteinopathy. (A) Neurons from non-diseased patients. (B) ALS neurons showing an increase in PFK transcript levels in response to mitochondrial defects (Barber and Shaw 2010). SV – synaptic vesicle.

Discussion

It is widely known that ALS patients display gross metabolic dysregulation described as hypermetabolism (for a recent review, see (Joardar, Manzo, and Zarnescu 2017). However, a major challenge in the field has been to understand how these clinical observations relate to metabolic changes at the cellular level. Here, we take advantage of cell type specific genetic tools available in *Drosophila* to pinpoint how specific metabolic changes in neurons and glia relate to disease progression. Using metabolic profiling we first found that the neuronal expression of TDP-43 increases the abundance of pyruvate, the end product of glycolysis. Notably, this alteration is consistent with metabolite changes in plasma from ALS patients (Lawton et al. 2012) and suggest an increase in glycolysis. Substantiating this scenario is transcriptional profiling of ALS spinal cords and patient derived iPSC motor neurons showing that just as in flies, PFK, the rate limiting step in glycolysis, is significantly upregulated (Fig. 2). Interestingly, metabolic profiling in flies also suggests increased glycolytic input into the pentose phosphate pathway (Supplemental Table 1), which provides a mechanism for countering oxidative stress via increased NADPH production (Kruger and von Schaewen 2003). Supporting this possibility are our findings that G6PD, the rate limiting enzyme of the pentose phosphate pathway is upregulated in fly and human ALS ventral and spinal cords, respectively (Fig. 2). Oxidative stress is a well-established ALS manifestation (Barber and Shaw 2010) and the most recent FDA approved drug for treating ALS patients, Radicava is aimed at countering this aspect of the disease (Cruz 2018). Collectively, molecular and metabolic alterations identified in the fly validate in patient derived motor neurons and spinal cords, albeit the magnitude of the changes found in human ALS tissues is often more dramatic and, at some level, more comparable with mutant TDP-43 dependent phenotypes in flies. These findings highlight the predictive power of the fly model and its relevance to studying disease pathomechanisms in humans.

Using a genetically encoded glucose sensor we show that TDP-43^{G298S} expressing motor neurons have increased capacity to import glucose (Fig. 3). This is consistent with increased glycolysis and its end product, pyruvate. It is unclear why despite finding that

329 pyruvate is also increased in motor neurons overexpressing TDP-43^{WT}, we could not detect
330 higher glucose uptake than in controls, although this is consistent with PFK transcript levels
331 trending up, yet not reaching significance in our data set (Fig. 2). A possible explanation is that
332 while our model is based on TDP-43 expression specifically in motor neurons or glia, the
333 metabolite profiling was performed on whole larvae and captured non-cell autonomous
334 changes, occurring in cells other than motor neurons. Nevertheless, taken together our data
335 show that there is a clear dysregulation of glycolysis in TDP-43 expressing *Drosophila* and
336 patient tissue samples. Alterations in glucose metabolism may also be a feature of multiple ALS
337 types. Indeed, pre-symptomatic SOD1 mutant mice have been shown to have high glucose
338 levels in spinal cords; however, glucose levels gradually decrease as disease symptoms
339 progress (Miyazaki et al. 2012). One question that remains is whether alterations in glucose
340 metabolism are compensatory or causative.

341 In an effort to address this question, we first increased glucose availability in *Drosophila*
342 by raising the dietary concentration of glucose (5-10 X higher than normal levels in standard fly
343 food), which mitigates locomotor defects and increases lifespan in ALS flies while making wild-
344 type larvae sluggish (Fig. 3). Interestingly, a high sugar diet only mitigates locomotor defects
345 when TDP-43 is expressed in motor neurons or glia but not muscles, indicating that the primary
346 metabolic defect lies in the nervous system and that muscles do not benefit from increased
347 glucose availability (Fig. 4 and Supplemental Figs. 4B and 4C). This is somewhat surprising
348 given that muscles normally rely on glycolysis for ATP production but is also consistent with
349 findings that in ALS, muscles switch to primarily using lipids and not glucose for energy
350 production (Palamiuc et al. 2015).

351 This systemic approach, however, does not provide information on which cells
352 specifically benefit from increased glucose availability. To answer this question, we intervened
353 genetically by overexpressing human glucose transporters GLUT-3 or GLUT-4 in motor
354 neurons, glia or muscles (Figs. 4-6 and Supplemental Figs. 4B and 4C). These experiments
355 showed that both GLUT-3 and GLUT-4 rescued locomotor dysfunction of TDP-43 expressing
356 larvae in the nervous system, but not in muscles (Fig. 4 and Supplemental Figs. 4B and 4C)

confirming our findings from high sugar feedings. Furthemore, our findings that overexpression of either GLUT-3 or GLUT-4 can help mitigate specific ALS-like phenotypes in flies are consistent with recent reports that both GLUT-3 and GLUT-4 are required at synapses to regulate activity (Ashrafi et al. 2017; Ferreira, Burnett, and Rameau 2011). Together, our dietary intervention and GLUT-3/4 overexpression experiments indicate that increased glucose availability in motor neurons and glia confers protection in models of TDP-43 proteinopathy, in a cell type dependent manner.

A possible explanation for why increased glucose availability improves defects caused by TDP-43 proteinopathy is that cells are actively consuming glucose to increase glycolytic flux. A recent study using vertebrate cell lines suggests that glycolytic flux depends on four key steps. They include: 1) glucose uptake by glucose transporters, 2) hexokinase levels, 3) PFK levels (and associated enzymes), and 4) lactate export, but not other enzymes or steps involved in glycolysis (Tanner et al. 2018). The co-over-expression of PFK mitigates TDP-43 defects in flies, and is consistent with our GLUT-3 over-expression experiments (Fig. 6). Surprisingly, PFK transcript levels were higher in human ALS post-mortem tissues compared to controls, however protein levels in total tissue homogenates were not significantly increased despite trending upwards (data not shown). Nevertheless, our findings of increased PFK mRNA levels in flies and human tissues, and the genetic interaction experiments support the notion that glycolysis is increased in ALS as a compensatory mechanism (see Figure 7 for model).

The fact that neurons would compensate deficits in cellular energetics through increasing glycolysis makes sense in the light of well-established defects in mitochondrial function. TDP-43 has been previously shown to localize to the inner mitochondrial membrane of mitochondria (Wang et al. 2016), and it has been shown to cause abnormally small mitochondria in *Drosophila* (Khalil et al. 2017). Consistent with the importance of glycolysis in neurodegeneration, there are reports of SNPs within PFK that are present in ALS patients but not in healthy controls (Rouillard et al. 2016; Xie et al. 2014). Our findings that glycolysis is increased as a compensatory mechanism and this confers neuroprotection is consistent with findings from a small clinical trial showing that a high caloric high carbohydrate diet improves

patient outcome (Wills et al. 2014b) and also that patients with diabetes have a later onset of disease (Kioumourtzoglou et al. 2015). While upregulation of glycolysis decreases the dependence of the organism for ATP derived from mitochondria, it is also possible that increased glycolysis is improving organismal health through a different mechanism. For example, pyruvate has been previously shown to protect mitochondria from oxidative stress (Wang et al. 2007). Future studies should focus on the link between glycolysis, oxidative stress and mitochondria in ALS.

Materials and Methods

Drosophila genetics

Standard crosses were incubated at 25°C with a 12-hour alternating dark-light cycles. (i) w^{1118} (ii) w^{1118}; UAS-TDP43^{WT}-YFP (iii) w^{1118}; UAS-TDP43^{G29S8}-YFP (iv)) UAS-GLUT3 flies were crossed with the GAL4 motor neuron driver D42. GLUT3 TDP-43 recombinant flies were generated using standard genetic techniques. GLUT3 flies were described in (Besson et al. 2015).

TDP-43 was expressed in motor neurons and glia using the D42 GAL4 (Gustafson and Boulianne 1996) and repo GAL4 (Sepp, Schulte, and Auld 2001) drivers, respectively. w^{1118} was crossed with either the D42 or repo GAL4 drivers as a control.

To manipulate PFK, we used w^{1118}; P{w[+mC]=UAS-Pfk.T}3 for over expression, and y^1 sc* v^1; P{y[+t7.7] v[+t1.8]=TRiP.HMS01324}attP2 or y^1 sc* v^1; P{y[+t7.7] v[+t1.8]=TRiP.GL00298}attP2 (Line 2, viable only in glial expressing flies) for PFK knock down. *attP2* was used as a genetic background control for PFK RNAi knock-down experiments. All lines were obtained from the Bloomington Stock Center.

PFK RNAi efficiency was assayed by crossing PFK RNAi to D42. Ventral nerve cords were dissected and analyzed via qPCR (see below for primers). A Welch's t-test was used to identify significance.

Fly food supplementation

Standard yeast/cornmeal/molasses food was heated and then allowed to cool to 55-60˚C. For high sugar supplementation, additional glucose was added to reach a final concentration of 357g/L (10X compared to regular food). Supplemented food was dispensed into vials and allowed to cool.

Locomotor assays

Larval turning assays were performed as previously described (Estes et al. 2011; Estes et al. 2013). Briefly, larvae are placed on a petri dish filled with solidified agar (2.5%) and grape juice. Third instar larvae are transferred from a vial onto the agar/juice surface and are allowed to acclimate. Using a clean paintbrush, larvae are turned ventral side up. The time it takes for larvae to turn themselves ventral side down and make a forward motion is recorded. Larval turning data were analyzed using Kruskal-Wallis multiple comparison tests (GraphPad Prism v7).

Metabolite analysis

Metabolomic analysis was conducted by Metabolon, Inc as previously described (Joardar et al. 2014; Manzo et al. 2018). Briefly, 50–60 wandering third instar larvae (~50–60 mg) per sample were collected and flash-frozen in liquid nitrogen. A total of 5 replicates per genotype were collected. Protein samples were analyzed by ultrahigh performance liquid chromatography/mass spectrometry (UHPLC/MS), or by gas chromatography/mass spectrometry (GC/MS). One-way ANOVA was used to identify biochemicals that differed significantly between experimental groups.

RNA isolation, cDNA preparation and qPCR

cDNA protocol has been previously described (Manzo et al. 2018). Briefly, 5 ventral nerve cords (VNCs) were isolated from third instar larvae per genotype using HL-3 saline buffer (70 mM NaCL, 5 mM KCl, 22 mM $MgCl_2$, 10 mM $NaHCO_3$, 5 mM trehalose, 115 mM sucrose, 5 mM

HEPES, pH 7.3). RNA was extracted using the RNeasy RNA Extraction Kit (Qiagen) and stored at -80°C. Genomic DNA (gDNA) was cleared using a DNase I (Thermo Fisher Scientific) digestion protocol. Following gDNA clearing, reverse transcription was performed using the Maxima First Strand cDNA Synthesis Kit for RT-qPCR (Thermo Fisher Scientific). The quality of the cDNA was tested using GPDH primers (see below for sequence) and GoTaq endpoint polymerase chain reaction (PCR) protocol (Promega). Quantitative PCR was performed using a SYBR Green protocol (Applied Biosystems) and primers designed to span exon-exon junctions. Each reaction was conducted in 3-6 biological replicates with three technical replicates each. ΔΔCT values are normalized to GPDH (Pfaffl 2001).The Kruskal-Wallis test was used to assess statistical significance in GraphPad Prism v7. Protocols for human tissue RNA isolation and cDNA preparation have been previously described (Bakkar et al. 2018). RT-PCR was performed using TaqMan Gene Expression Assays following the TaqMan Fast Advanced Master Mix protocol (Applied Biosystems) on the QuantStudio 6 Flex instrument (Applied Biosystems).

Primer sequences and Taqman probes

Drosophila Phosphofructokinase (PFK): Forward primer - TGGACGAGCTGGTCAAGAAC; Reverse primer - CCACAAGAGCTAAATAGCCG

Drosophila G6PD (Zw): Forward primer - AAGCGCCGCAACTCTTTG; Reverse primer - AGGGCGGTGTGATCTTCC

Drosophila GPDH: Forward primer - CCGCAGTGCTTGTTTTGCT*;* Reverse primer – TATGGCCGAACCCCAGTTG

Human *Phosphofructokinase P* (PFKP): Assay ID Hs00242993_m1

Human *Phosphofructokinase M* (PFKM): Assay ID Hs00175997_m1

Human G6PD: Assay ID Hs00166169_m1

Human GAPDH: Assay ID Hs99999905_m1

Glucose sensor

Third instar larval brains where dissected in HL3-buffer (70 mM NaCl, 5 mM KCl, 20 mM MgCl2, 10 mM NaHCO3, 115 mM sucrose, 5 mM trehalose, 5 mM HEPES; pH 7.1). Of note, the glucose sensor is not sensitive to trehalose (Volkenhoff et al. 2018). Larvae were pinned down on a Sylgard plate using insect pins and cleaned so that the ventral nerve cord is clearly visible. A 40x water immersion lens was used to image larvae individually. For glucose stimulation, HL3-buffer was removed and replaced with 5mM glucose supplemented HL3 (70 mM NaCl, 5 mM KCl, 20 mM MgCl2, 10 mM NaHCO3, 115 mM sucrose, 5 mM glucose, 5mM HEPES, pH 7.1).

Fluorescent images were acquired using a Zeiss LSM880 NLO upright multiphoton/confocal microscope. CFP was excited using a 405-nm laser, and images were acquired in both the CFP (CFP 465–499 nm) and the FRET (535–695 nm) detection channels.

Data was analyzed using ImageJ with a drift correction plugin turboreg (Thevenaz, Ruttimann, and Unser 1998). Regions of interest (ROIs) were manually selected and the mean grey value of each ROI was extracted. The mean grey values for the FRET and CFP channels was taken to calculate the FRET ratio (F/C), which corresponds to the intracellular glucose concentration.

Each ROI was imaged every 10 seconds for 10 minutes (baseline) and then for another 10 minutes under high glucose HL-3 (stim). Each FRET ratio was normalized to the mean baseline value for each genotype. For baseline vs stim comparisons (Fig. 3B), the normalized FRET ratio of each ROI was taken from minutes 5-10 and minutes 15-20.

FM1-43 experiments

Larvae are dissected in HL-3 buffer on a sylgard dish as previously described. FM1-43 dye uptake assays were conducted using 4 μM FM1-43FX, 90 mM KCl, and 2 mM Ca2+ for stimulation. Methods adapted from (Verstreken, Ohyama, and Bellen 2008; Kuromi and Kidokoro 2005). To determine dye uptake signal, the background-corrected fluorescence for

every synaptic bouton was calculated by subtracting the mean background fluorescence of cell-free regions equal in size to the synaptic bouton.

Bouton counts

Larval NMJs were dissected and fixed with 3.5% paraformaldehyde in PBS (pH 7.2: 130 mM NaCl, 5 mM Na_2HPO_4, 5mM NaH_2PO_4) for 30 minutes. Antibody dilutions are as follows: 1:300 mouse anti-DCSP2 (DSHB), 1:500 anti-mouse Alexa Fluor 568 (Invitrogen), 1:200 Anti-HRP-CY5 conjugate (Invitrogen), and 1:40 Phalloidin-488 (Invitrogen). Blocking solution contained 2% BSA and 5% Normal goat serum. Methods have been previously described in (Coyne et al. 2014).

Larval muscles 6 and 7, segment A3, were imaged using an LSM 880 confocal microscope (Zeiss). NIH ImageJ was used to count bouton numbers and measure muscle area. Bouton count was normalized to muscle area to account for size variation.

iPSC methods

Control iPSC and TDP-43 iPSC cells were differentiated to motor neurons as previously described (Donnelly et al. 2013; Zhang et al. 2015).

Statistics

All statistical analyses for locomotor assays or qPCR comprising three or more data sets were conducted using Kruskal-Wallis with uncorrected Dunn's test in Prism v8.0 (GraphPad). When only two data sets were compared, either Welch's test or Wilcoxon signed-rank test were used.

References cited:

Ashrafi, G., Z. Wu, R. J. Farrell, and T. A. Ryan. 2017. 'GLUT4 Mobilization Supports Energetic Demands of Active Synapses', *Neuron*, 93: 606-15 e3.

Bakkar, N., T. Kovalik, I. Lorenzini, S. Spangler, A. Lacoste, K. Sponaugle, P. Ferrante, E. Argentinis, R. Sattler, and R. Bowser. 2018. 'Artificial intelligence in neurodegenerative

disease research: use of IBM Watson to identify additional RNA-binding proteins altered in amyotrophic lateral sclerosis', *Acta Neuropathol*, 135: 227-47.

Barber, S. C., and P. J. Shaw. 2010. 'Oxidative stress in ALS: key role in motor neuron injury and therapeutic target', *Free Radic Biol Med*, 48: 629-41.

Besson, M. T., K. Alegria, P. Garrido-Gerter, L. F. Barros, and J. C. Lievens. 2015. 'Enhanced neuronal glucose transporter expression reveals metabolic choice in a HD Drosophila model', *PLoS ONE*, 10: e0118765.

Browne, S. E., L. Yang, J. P. DiMauro, S. W. Fuller, S. C. Licata, and M. F. Beal. 2006. 'Bioenergetic abnormalities in discrete cerebral motor pathways presage spinal cord pathology in the G93A SOD1 mouse model of ALS', *Neurobiol Dis*, 22: 599-610.

Coyne, A. N., I. Lorenzini, C. C. Chou, M. Torvund, R. S. Rogers, A. Starr, B. L. Zaepfel, J. Levy, J. Johannesmeyer, J. C. Schwartz, H. Nishimune, K. Zinsmaier, W. Rossoll, R. Sattler, and D. C. Zarnescu. 2017. 'Post-transcriptional Inhibition of Hsc70-4/HSPA8 Expression Leads to Synaptic Vesicle Cycling Defects in Multiple Models of ALS', *Cell reports*, 21: 110-25.

Coyne, A. N., B. B. Siddegowda, P. S. Estes, J. Johannesmeyer, T. Kovalik, S. G. Daniel, A. Pearson, R. Bowser, and D. C. Zarnescu. 2014. 'Futsch/MAP1B mRNA Is a Translational Target of TDP-43 and Is Neuroprotective in a Drosophila Model of Amyotrophic Lateral Sclerosis', *J Neurosci*, 34: 15962-74.

Cruz, M. P. 2018. 'Edaravone (Radicava): A Novel Neuroprotective Agent for the Treatment of Amyotrophic Lateral Sclerosis', *P T*, 43: 25-28.

Donnelly, C. J., P. W. Zhang, J. T. Pham, A. R. Haeusler, N. A. Mistry, S. Vidensky, E. L. Daley, E. M. Poth, B. Hoover, D. M. Fines, N. Maragakis, P. J. Tienari, L. Petrucelli, B. J. Traynor, J. Wang, F. Rigo, C. F. Bennett, S. Blackshaw, R. Sattler, and J. D. Rothstein. 2013. 'RNA toxicity from the ALS/FTD C9ORF72 expansion is mitigated by antisense intervention', *Neuron*, 80: 415-28.

Dupuis, L., P. F. Pradat, A. C. Ludolph, and J. P. Loeffler. 2011. 'Energy metabolism in amyotrophic lateral sclerosis', *Lancet Neurol*, 10: 75-82.

Estes, P. S., A. Boehringer, R. Zwick, J. E. Tang, B. Grigsby, and D. C. Zarnescu. 2011. 'Wild-type and A315T mutant TDP-43 exert differential neurotoxicity in a Drosophila model of ALS', *Human Molecular Genetics*, 20: 2308-21.

Estes, P. S., S. G. Daniel, A. P. McCallum, A. V. Boehringer, A. S. Sukhina, R. A. Zwick, and D. C. Zarnescu. 2013. 'Motor neurons and glia exhibit specific individualized responses to TDP-43 expression in a Drosophila model of amyotrophic lateral sclerosis', *Disease models & mechanisms*, 6: 721-33.

Fehr, M., S. Lalonde, I. Lager, M. W. Wolff, and W. B. Frommer. 2003. 'In vivo imaging of the dynamics of glucose uptake in the cytosol of COS-7 cells by fluorescent nanosensors', *J Biol Chem*, 278: 19127-33.

Ferreira, J. M., A. L. Burnett, and G. A. Rameau. 2011. 'Activity-dependent regulation of surface glucose transporter-3', *J Neurosci*, 31: 1991-9.

Gustafson, K., and G. L. Boulianne. 1996. 'Distinct expression patterns detected within individual tissues by the GAL4 enhancer trap technique', *Genome*, 39: 174-82.

Hardiman, O., A. Al-Chalabi, A. Chio, E. M. Corr, G. Logroscino, W. Robberecht, P. J. Shaw, Z. Simmons, and L. H. van den Berg. 2017. 'Amyotrophic lateral sclerosis', *Nat Rev Dis Primers*, 3: 17071.

Joardar, A., E. Manzo, and D. C. Zarnescu. 2017. 'Metabolic Dysregulation in Amyotrophic Lateral Sclerosis: Challenges and Opportunities', *Curr Genet Med Rep*, 5: 108-14.

Joardar, A., J. Menzl, T. C. Podolsky, E. Manzo, P. S. Estes, S. Ashford, and D. C. Zarnescu. 2014. 'PPAR gamma activation is neuroprotective in a Drosophila model of ALS based on TDP-43', *Hum Mol Genet*.

Khalil, B., M. J. Cabirol-Pol, L. Miguel, A. J. Whitworth, M. Lecourtois, and J. C. Lievens. 2017. 'Enhancing Mitofusin/Marf ameliorates neuromuscular dysfunction in Drosophila models of TDP-43 proteinopathies', *Neurobiology of aging*, 54: 71-83.

Kioumourtzoglou, M. A., R. S. Rotem, R. M. Seals, O. Gredal, J. Hansen, and M. G. Weisskopf. 2015. 'Diabetes Mellitus, Obesity, and Diagnosis of Amyotrophic Lateral Sclerosis: A Population-Based Study', *JAMA Neurol*, 72: 905-11.

Kruger, N. J., and A. von Schaewen. 2003. 'The oxidative pentose phosphate pathway: structure and organisation', *Curr Opin Plant Biol*, 6: 236-46.

Kuromi, H., and Y. Kidokoro. 2005. 'Exocytosis and endocytosis of synaptic vesicles and functional roles of vesicle pools: lessons from the Drosophila neuromuscular junction', *The Neuroscientist : a review journal bringing neurobiology, neurology and psychiatry*, 11: 138-47.

Lawton, K. A., M. E. Cudkowicz, M. V. Brown, D. Alexander, R. Caffrey, J. E. Wulff, R. Bowser, R. Lawson, M. Jaffa, M. V. Milburn, J. A. Ryals, and J. D. Berry. 2012. 'Biochemical alterations associated with ALS', *Amyotrophic lateral sclerosis : official publication of the World Federation of Neurology Research Group on Motor Neuron Diseases*, 13: 110-8.

Ling, S. C., M. Polymenidou, and D. W. Cleveland. 2013. 'Converging mechanisms in ALS and FTD: disrupted RNA and protein homeostasis', *Neuron*, 79: 416-38.

Ludolph, A. C., K. J. Langen, M. Regard, H. Herzog, B. Kemper, T. Kuwert, I. G. Bottger, and L. Feinendegen. 1992. 'Frontal lobe function in amyotrophic lateral sclerosis: a neuropsychologic and positron emission tomography study', *Acta neurologica Scandinavica*, 85: 81-9.

Manzo, E., A. G. O'Conner, J. M. Barrows, D. D. Shreiner, G. J. Birchak, and D. C. Zarnescu. 2018. 'Medium-Chain Fatty Acids, Beta-Hydroxybutyric Acid and Genetic Modulation of the Carnitine Shuttle Are Protective in a Drosophila Model of ALS Based on TDP-43', *Front Mol Neurosci*, 11: 182.

Mergenthaler, P., U. Lindauer, G. A. Dienel, and A. Meisel. 2013. 'Sugar for the brain: the role of glucose in physiological and pathological brain function', *Trends Neurosci*, 36: 587-97.

Miyazaki, K., K. Masamoto, N. Morimoto, T. Kurata, T. Mimoto, T. Obata, I. Kanno, and K. Abe. 2012. 'Early and progressive impairment of spinal blood flow-glucose metabolism coupling in motor neuron degeneration of ALS model mice', *J Cereb Blood Flow Metab*, 32: 456-67.

Musselman, L. P., J. L. Fink, K. Narzinski, P. V. Ramachandran, S. S. Hathiramani, R. L. Cagan, and T. J. Baranski. 2011. 'A high-sugar diet produces obesity and insulin resistance in wild-type Drosophila', *Dis Model Mech*, 4: 842-9.

Na, J., L. P. Musselman, J. Pendse, T. J. Baranski, R. Bodmer, K. Ocorr, and R. Cagan. 2013. 'A Drosophila model of high sugar diet-induced cardiomyopathy', *PLoS Genet*, 9: e1003175.

Neumann, M., D. M. Sampathu, L. K. Kwong, A. C. Truax, M. C. Micsenyi, T. T. Chou, J. Bruce, T. Schuck, M. Grossman, C. M. Clark, L. F. McCluskey, B. L. Miller, E. Masliah, I. R. Mackenzie, H. Feldman, W. Feiden, H. A. Kretzschmar, J. Q. Trojanowski, and V. M. Lee. 2006. 'Ubiquitinated TDP-43 in frontotemporal lobar degeneration and amyotrophic lateral sclerosis', *Science*, 314: 130-3.

Palamiuc, L., A. Schlagowski, S. T. Ngo, A. Vernay, S. Dirrig-Grosch, A. Henriques, A. L. Boutillier, J. Zoll, A. Echaniz-Laguna, J. P. Loeffler, and F. Rene. 2015. 'A metabolic switch toward lipid use in glycolytic muscle is an early pathologic event in a mouse model of amyotrophic lateral sclerosis', *EMBO molecular medicine*, 7: 526-46.

Pfaffl, M. W. 2001. 'A new mathematical model for relative quantification in real-time RT-PCR', *Nucleic acids research*, 29: e45.

Rouillard, A. D., G. W. Gundersen, N. F. Fernandez, Z. Wang, C. D. Monteiro, M. G. McDermott, and A. Ma'ayan. 2016. 'The harmonizome: a collection of processed datasets gathered to serve and mine knowledge about genes and proteins', *Database : the journal of biological databases and curation*, 2016.

Sepp, K. J., J. Schulte, and V. J. Auld. 2001. 'Peripheral glia direct axon guidance across the CNS/PNS transition zone', *Dev Biol*, 238: 47-63.

Takanaga, H., B. Chaudhuri, and W. B. Frommer. 2008. 'GLUT1 and GLUT9 as major contributors to glucose influx in HepG2 cells identified by a high sensitivity intramolecular FRET glucose sensor', *Biochim Biophys Acta*, 1778: 1091-9.

Tanner, L. B., A. G. Goglia, M. H. Wei, T. Sehgal, L. R. Parsons, J. O. Park, E. White, J. E. Toettcher, and J. D. Rabinowitz. 2018. 'Four Key Steps Control Glycolytic Flux in Mammalian Cells', *Cell Syst*, 7: 49-62 e8.

Tauffenberger, A., A. Vaccaro, A. Aulas, C. Vande Velde, and J. A. Parker. 2012. 'Glucose delays age-dependent proteotoxicity', *Aging cell*.

Teyssou, Elisa and Chartier Laura and Amador Maria-Del-Mar and Lam Roselina and Lautrette Graldine and Nicol Marie and Machat Selma and. 2017. 'Novel UBQLN2 mutations linked to amyotrophic lateral sclerosis and atypical hereditary spastic paraplegia phenotype through defective HSP70-mediated proteolysis.', *Neurobiology of aging*, 58: 239.e11--39.e20.

Thevenaz, P., U. E. Ruttimann, and M. Unser. 1998. 'A pyramid approach to subpixel registration based on intensity', *IEEE Trans Image Process*, 7: 27-41.

Verstreken, P., T. Ohyama, and H. J. Bellen. 2008. 'FM 1-43 labeling of synaptic vesicle pools at the Drosophila neuromuscular junction', *Methods Mol Biol*, 440: 349-69.

Volkenhoff, A., J. Hirrlinger, J. M. Kappel, C. Klambt, and S. Schirmeier. 2018. 'Live imaging using a FRET glucose sensor reveals glucose delivery to all cell types in the Drosophila brain', *J Insect Physiol*, 106: 55-64.

Wang, W., L. Wang, J. Lu, S. L. Siedlak, H. Fujioka, J. Liang, S. Jiang, X. Ma, Z. Jiang, E. L. da Rocha, M. Sheng, H. Choi, P. H. Lerou, H. Li, and X. Wang. 2016. 'The inhibition of TDP-43 mitochondrial localization blocks its neuronal toxicity', *Nat Med*, 22: 869-78.

Wang, X., E. Perez, R. Liu, L. J. Yan, R. T. Mallet, and S. H. Yang. 2007. 'Pyruvate protects mitochondria from oxidative stress in human neuroblastoma SK-N-SH cells', *Brain Res*, 1132: 1-9.

Wills, A. M., J. Hubbard, E. A. Macklin, J. Glass, R. Tandan, E. P. Simpson, B. Brooks, D. Gelinas, H. Mitsumoto, T. Mozaffar, G. P. Hanes, S. S. Ladha, T. Heiman-Patterson, J. Katz, J. S. Lou, K. Mahoney, D. Grasso, R. Lawson, H. Yu, M. Cudkowicz, and M. D. A. Clinical Research Network. 2014a. 'Hypercaloric enteral nutrition in patients with

amyotrophic lateral sclerosis: a randomised, double-blind, placebo-controlled phase 2 trial', *Lancet*, 383: 2065-72.

———. 2014b. 'Hypercaloric enteral nutrition in patients with amyotrophic lateral sclerosis: a randomised, double-blind, placebo-controlled phase 2 trial', *Lancet*, 383: 2065-72.

Xie, T., L. Deng, P. Mei, Y. Zhou, B. Wang, J. Zhang, J. Lin, Y. Wei, X. Zhang, and R. Xu. 2014. 'Genome-wide association study combining pathway analysis for typical sporadic amyotrophic lateral sclerosis in Chinese Han populations', *Neurobiology of aging*, 35: 1778 e9-78 e23.

Zhang, P. W., A. M. Haidet-Phillips, J. T. Pham, Y. Lee, Y. Huo, P. J. Tienari, N. J. Maragakis, R. Sattler, and J. D. Rothstein. 2015. 'Generation of GFAP::GFP astrocyte reporter lines from human adult fibroblast-derived iPS cells using zinc-finger nuclease technology', *Glia*.